High-purity synthesis of La2SiO5 by solid-state reaction between La2O3 and different characteristics of SiO2

Lizeth Arbelaez, Pierre-Marie Geffroy, Anne Aimable, Koichiro Fukuda, Emilie Béchade

High-purity synthesis of La_2SiO_5 by solid-state reaction between La_2O_3 and different characteristics of SiO_2

Lizeth Arbelaez[a,*], Pierre-Marie Geffroy[a], Anne Aimable[a], Koichiro Fukuda[b], Emilie Béchade[a]

[a]*Université de Limoges, IRCER, CNRS, UMR 7315, 12 Rue Atlantis, F-87000 Limoges, France*

[b]*Department of Life Science and Applied Chemistry, Nagoya Institute of Technology, Nagoya 466-8555, Japan*

*Corresponding author

E-mail address: lizeth.arbelaez-morales@unilim.fr

Abstract

The solid-state reaction between lanthanum oxide and different characteristics of silica has been investigated to define new process conditions that favor the formation of La_2SiO_5 and to characterize the La_2O_3: SiO_2 reaction mechanisms. Silica with different crystalline structures (amorphous or quartz-type silica) and various average particle sizes of ~36, 12, 1, and 0.02 µm were used. The 1:1 M ratio mixtures between La_2O_3 and different types of SiO_2 were ground and subsequently heated at 1200 and 1500°C for 10 h. The morphology of the ground mixtures, their thermal properties, and the phases obtained after heating were determined in this study. The phases identified after each solid-state synthesis were quantified using Rietveld refinements. The results obtained indicate that an amorphous silica with a small particle size (<1 µm) is more advantageous in the La_2SiO_5 powder synthesis. An

alternative synthesis method of using an amorphous colloidal silica with a particle size of 0.02 µm is proposed, and the purity level achieved at 1500°C after 10 h is higher than 90 vol%. A reaction mechanism was suggested that highlights the strong effect of the size ratio (La_2O_3/SiO_2: 1 µm/0.02 µm) to improve the reactivity and La_2SiO_5 phase formation.

Keywords: La_2SiO_5 synthesis, solid-state reaction, silica particle size, reaction mechanism

1 Introduction

Lanthanum orthosilicate (La_2SiO_5), lanthanum disilicate $La_2Si_2O_7$, and oxyapatite ($La_{9.33+x}(SiO_4)_6O_{2+3x/2}$) are three compounds that can be formed according to the phase diagram of the La_2O_3-SiO_2 system [1]. However, lanthanum monosilicate La_2SiO_5 has interesting applications in the field of optics, ceramics, electronics and procedures that require good resistance to abrasion and high temperatures [2–4] due to its crystal structure and physical-chemical properties. La_2SiO_5 has a monoclinic unit cell of the P21/C space group, and its atomic structure contains both isolated SiO_4 tetrahedra and nonsilicon bonded oxygen atoms [5]. Thus, this material is also known by the name of oxyorthosilicate, and its chemical formula can be rewritten as $La_2(SiO)_4O$ [6,7]. Moreover, Fukuda et al. [8–10] have used this lanthanum silicate to obtain a highly c-axis oriented apatite-type lanthanum silicate by reactive diffusion between sandwich-type layers of La_2SiO_5 and $La_2Si_2O_7$. Likewise, other sandwich-type layer combinations such as La_2SiO_5/SiO_2 [11] and La_2SiO_5/B_2O_3 vapors [12] have been proposed with successful results in apatite orientation. Generally, the

La_2SiO_5 compound must be of high purity for this type of applications, but few studies documented adequate requirements to synthesize lanthanum monosilicate in the literature.

The usual reported method for La_2SiO_5 phase synthesis (or other rare earth silicates, RE: Rare Earth) consists of a solid-state reaction between La_2O_3 (or RE_2O_3) and SiO_2 powders [3,6,7,13–17]. The characteristics of the silica powder reagents, such as the particle size and silica crystallinity, are seldom mentioned. For the La_2SiO_5 synthesis authors such as Fukuda et al. [8,18] have used crystalline silica (quartz type-silica >99.0%) contrarily, Tzvetkov et al. have used amorphous silica [4]. For the synthesis and structure investigations of the rare-heart silicate phases, A. Christensen et al. [13] used amorphous silica known as kieselguhr or diatomite, which has a high amount of impurities such as Al_2O_3, MgO, and Fe_2O_3 [19]. Usually, the studies related to the synthesis of rare earth silicates have in common the use of high-purity silica powders (>99.0%) [4,5,8,12,13,15,16,20–22]. Due to the low reactions between La_2O_3 and SiO_2, the synthesis by solid-state reaction of this type of materials broadly requires high temperatures (1400-1700°C), long sintering time (20-200 h), and alternated grinding cycles [13,23–30]. Because of the poor homogenization of the starting materials, local variations in stoichiometric mixtures can be generated and cause the formation of other compounds of the $RE_2O_3 – SiO_2$ system [13,22,26,31]. In the case of the synthesis of La_2SiO_5 with 1:1 molar ratio, secondary phases such as $La_{9.33+x}(SiO_4)_6O_{2+3x/2}$ (7:9 M ratio) and $La_2Si_2O_7$ (1:2 M ratio) were observed. Notwithstanding, Brandle et al. have reported that at high temperatures some RE_2SiO_5 phases (including La_2SiO_5) can decompose into the respective rare earth oxide (RE_2O_3) and a higher silicate, which is believed to be the

apatite and $La_2Si_2O_7$ phase [20]. Different alternatives have been proposed to reduce the synthesis temperatures of rare earth silicates. Leskela et al. [7] used flux materials to accelerate the rare earth silicate synthesis reaction and limited the decomposition of RE_2SiO_5 at high temperature. Other authors have used low-temperature techniques such as sol-gel synthesis and mechanochemical methods [4,32–38]. G. Tzvetkov et al. [4] proposed a mechanochemical method to synthesize lanthanum monosilicate La_2SiO_5. In this case, after La_2O_3 and SiO_2 were milled in 4:3 M ratio, an apatite $La_{4.67}(SiO_4)_3O$ powder precursor was formed during the heat treatment at approximately 880°C. By heating the latter powder at 1100°C for 2 h, the La_2SiO_5 phase was obtained. The gradual amorphization of the reagents and the formation of a silicate precursor enable one to considerably reduce the synthesis temperature [37,39,40]. In addition, this method is reported to be promising in the complex oxide synthesis, when the starting powders are hydroxides or hydrated oxides (highly hygroscopic), as in the case of La_2O_3 [38,41,42]. In contrast, the synthesis of rare earth silicates by the solid-state method has difficulty in obtaining a single phase. However, considering industrial applications, solid-state reaction processes have advantages because they are relatively simple to implement, which enables the production of a large amount of powders.

In all of the aforementioned papers, the conditions for the solid-state reaction were not always clearly expressed. The milling step of the starting powders, silica crystallinity/property particle size, and La_2O_3/SiO_2 particle size ratio can strongly affect the final purity of the La_2SiO_5 phase. For the Y_2O_3-Al_2O_3 system in the $Y_3Al_5O_{12}$ (YAG) synthesis, it has been reported that the solid-state reaction and kinetics pathways are drastically impacted by the particle size and size ratio of the

reagents [43]. Additionally, if the diffusion rate of the system is slow, and nearby contacts between the particles of the components are not provided, the reaction efficiency will be low [37,38,42].

This work aims to provide a better understanding of the La_2SiO_5 phase formation during the solid-state reaction at high temperature. Hence, the impacts of the characteristics of the starting powder, particularly the silica crystallinity, particle size, and size ratio La_2O_3/SiO_2, have been studied. A reaction mechanism through the solid-state treatment and supported by a thermodynamic analysis was proposed, which highlights the strong effect of the size ratio (La_2O_3/SiO_2: 1 µm/0.002 µm) to improve the reactivity and La_2SiO_5 phase formation.

2 Experimental methods

2.1. Protocol of the synthesis of La_2SiO_5 powder by the solid-state reaction

Lanthanum silicate La_2SiO_5 powders were prepared by a solid-state reaction using high-purity powders of amorphous silica (Prolabo, > 99.5%), crystalline silica (quartz-type silica: C- 400, 98.73%) and colloidal silica (monodisperse amorphous silica 40 wt. % in H_2O: LUDOX AS-40) with different particle sizes. La_2O_3 (99.9% Sigma Aldrich) was used as the source of lanthanum. La_2O_3 was previously dried at 1100°C in 1 h to eliminate lanthanum hydroxide and/or oxycarbonates and to determine the appropriate amount of this reagent. According to the phase diagram, La_2O_3 and SiO_2

were mixed in 1:1 molar ratio to obtain La_2SiO_5. The mass of the reaction mixture was approximately 15 g for each synthesis (12.67 g of La_2O_3 and 2.34 g of SiO_2).

Amorphous and crystalline quartz-type silica powders were milled with La_2O_3 powder by attrition (Union Procces-Szegvari attritor system) in distilled water in 2.5 h at 450 rpm in a Teflon bowl with zirconia balls of 1 mm and 2 mm in diameter.

In the case of colloidal silica (provided as an aqueous suspension 40 wt.%), 5.85 g of silica suspension was first added with 40 mL of distilled water and dispersed in a 100-mL glass beaker. The dispersion was done using an ultrasonic pulsing method with a sonotrode Vibra-Cell$^{T.M.}$ (Bioblock Scientific Co, Ltd, Illkirich, France). The dispersion conditions were fixed to an amplitude of 65% with cycles of 10 seconds on and 5 seconds off in 2 min. The sonotrode was rinsed with distilled water after each session. Then, 12.67 g of La_2O_3 powder was added to the silica suspension, and the mixture was dispersed again with ultrasons. Afterwards, distilled water was added to fill the beaker to 70 mL. The mixture was rapidly put on a heating plate under stirring at 450 rpm using a magnetic stirrer and at a temperature of 160°C until the water completely evaporated to obtain a homogeneous and dry powder.

All powders after milling and/or dispersion by the ultrasonic method were dried overnight at 110°C in air. Then, the dried mixing powders were crushed using an agate mortar to break the agglomerates that formed after drying and homogenize before calcination. Finally, the dried powders were calcined using an oven TERMOLAB (Fornos Eléctricos. Lda, Águeda, Portugal) in Pt crucibles at 1200°C and 1500°C for 10 h in air at a heating rate of 10°Cmin^{-1}.

The synthesis results obtained by mixing lanthanum oxide (L) and silica (S) powders are denoted with LS. The latter is followed by the type of silica (a: amorphous; q:

crystalline; c: colloidal) and average silica particle size (µm), as reported in Table 1. For example, the powder denoted by LSa_{36} corresponds to a mixture of lanthanum oxide and amorphous silica with an average particle size of 36 micrometers.

2.2. Characterization methods

The particle sizes of the silica powders were measured using a Model LA-950V2 Fraunhofer scientific analyzer (Horiba, Kyoto, Japan). The specific surface areas of the powders were determined using Brunauer Emmett Teller (BET) after degassing in vacuum at 200°C. Microstructural analysis was performed by scanning electron microscopy (SEM-FEG LEO1530 VP); the samples were previously metallized by a thin layer of carbon.

The thermal behavior of the starting mixtures of La_2O_3 (L) and different types of SiO_2 (S) in 1:1 molar ratio were analyzed by thermogravimetric and differential scanning calorimetry analysis (TG-DSC) using a NETZSCH STA 449 F3 Jupiter analyzer. The experiments were performed under an air flow of 20 mL/min with rise and fall temperature ramps of 10°C/min to 1500°C.

The powders obtained by the solid-state reaction were characterized by X-ray diffraction (Bruker D8 Advance diffractometer (Germany), 2θ-θ mode, CuK_α radiation) in the 2θ range of 10-60° (step size: 0.02°; time range: 30 min). Likewise, to better understand the formation of La_2SiO_5 throughout the solid-state reaction, *in situ* high-temperature XRD was performed on the starting mixtures at 100°C increments in the temperature range of 600-1150°C. The heating rate from room temperature was 10°C min^{-1}. The crystalline phases were identified using the Joint Committee on

Powder Diffraction Standards–Inorganic Crystal Structure Database (JCPDS–ICSD). The ICSD database in this study are shown in Table 1. The crystallized phases were quantified by Rietveld method of the HighScore Plus software using polynomial background.

Table 1. *Crystallized phases during the solid-state reaction of the LS mixtures*

Phase	N°JCPDS	Space Group	Crystal lattice
SiO_2 Cristobalite	98-007-5484 [35]	P 41 21 2	Tetragonal
La_2O_3	98-002-8555 [36]	P 6_3/m m c	Hexagonal
La_2SiO_5	98-015-7892 [20]	P 1 21/c 1	Monoclinic
$La_{9,33}(SiO_4)_6O_2$	98-015-4068 [37]	P 6_3/m	Hexagonal
$La_2Si_2O_7$	98-007-1807 [38]	P 1 21/c 1	Monoclinic

3 Results and discussion

3.1. Effect of the crystallinity of the silica starting powders on the La_2SiO_5 synthesis

In this section, it is assumed that the nature of the silica powders significantly affects the kinetics of formation of the La_2SiO_5 phase at high temperature. Hence, La_2SiO_5 was synthesized using two different starting powders of silica: one amorphous (LSa_{36}) and another with crystalline structure (type quartz, LSq_{12}). Mixtures of La_2O_3 and silica were milled and calcined at two different temperatures (1200°C and 1500°C) for 10 h. The XRD diagrams presented in Figure 1, show that $La_{9,33+2x}(SiO_4)_6O_{2+3x}$ (Ap), and La_2SiO_5 phases are identified as the main compounds in all synthesized powders. In Tables 2, Table 3, the phase quantification obtained by Rietveld method reveals that the oxyapatite Ap (the exact stoichiometry composition is unknown) is mostly promoted when crystalline silica is used as the starting reagent (64.7% at 1200°C and 60.7% at 1500 °C for LSq_{12}). A significant amount of

unreacted La_2O_3 is observed especially in the LSa_{36} sample after the heat treatment at 1200°C. However, the Rietveld analysis shows that the La_2O_3 phase ratio (%Vol) decreases from 11% to 9.8% from 1200°C to 1500°C for LSa_{36} powder. La_2O_3 has almost completely disappeared at 1500°C in the LSq_{12} sample. In contrast, SiO_2 is completely consumed by the reaction in LSa_{36} powders from 1200°C, whereas 2.9% of silica in the form of cristobalite is detected in LSq_{12} powders calcined at 1500°C. Meanwhile, traces of $La_2Si_2O_7$ are only observed in LSa_{36} powders: 1.2% is detected at 1200°C, and this compound continues to grow with increasing temperature. Therefore, at 1500°C, the amount of this compound increased to 6.6%.

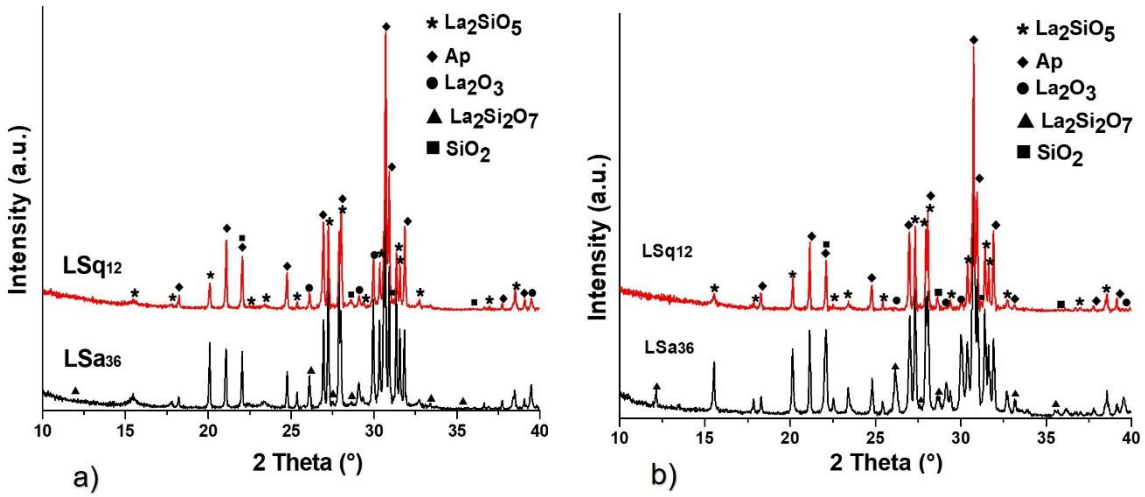

***Figure 1**. XRD patterns of LSq12 and LSa36 samples calcined at a) 1200 °C/10 h and b) 1500 °C/10 h.*

There appears to be a relationship between the silica crystallinity and the phases produced during the solid-state reaction at high temperature. The amount of lanthanum orthosilicate obtained from the LSa_{36} sample after calcination process at 1500°C during 10 h was 46.7%, which is the highest value in this part of the study (see Table 3). This shows that amorphous silica is more advantageous for the purity of the La_2SiO_5 phase. Moreover, crystalline quartz-type silica probably benefits the

formation of the apatite phase, since it is obtained in high proportions after the solid-state synthesis of LSq12 powders (see Table 2). It can be explained by the crystalline structure of the quartz-type silica, which is hexagonal and possibly promotes the apatite crystallization at the expense of La_2SiO_5 formation (apatite is also hexagonal, Table 1). Nevertheless, the purity of the La_2SiO_5 phase using an amorphous silica remains very low (below 50%), and the synthesis is not optimized because it has a great amount of unreacted La_2O_3.

Table 2. *Phase quantification of LSq_{12} and LSa_{36} samples calcined at 1200°C/10h by the Rietvel method*

Syntheses at 1200°C	**Size ratio** $R = \frac{d\,La2O3}{d\,SiO2}$	**La_2SiO_5 %**	**Apatite %**	**$La_2Si_2O_7$ %**	**La_2O_3 %**	**SiO_2 %**
LSa_{36}	$^{1\mu m}/_{36\mu m}$	45.5	42.3	1.2	11	-
LSq_{12}	$^{1\mu m}/_{12\mu m}$	27.0	64.7	-	5.1	3.3

Table 3. *Phase quantification of LSq_{12} and LSa_{36} samples calcined at 1500°C/10h by the Rietveld method*

Syntheses at 1500°C	**Size ratio** $R = \frac{d\,La2O3}{d\,SiO2}$	**La_2SiO_5 %**	**Apatite %**	**$La_2Si_2O_7$ %**	**La_2O_3 %**	**SiO_2 %**
LSa_{36}	$^{1\mu m}/_{36\mu m}$	46.7	37.1	6.6	9.8	-
LSq_{12}	$^{1\mu m}/_{12\mu m}$	36.3	60.2	-	0.6	2.9

3.2. Effect of the particle size of silica starting powders on the La_2SiO_5 synthesis

3.2.1. Properties of the starting powders

Table 4 shows the average particle size and specific surface area for the starting reagents. The silica with an average particle size of 36 µm was ground to obtain the amorphous silica with an average size of 1 µm. The specific surface area of colloidal silica is given by the provider. The usual notations for each reagents are also provided in Table 4. SEM micrographs of the starting silica and lanthanum oxide powders are presented in Figure 2.

***Table 4**. Characteristics of the starting powders*

Raw material	Average particle size (µm)	SBET (m^2/g)	Starting powder name reference
Amorphous silica	36	0.61 ±0.03	Sa_{36}
Amorphous silica	1	16 ± 0.01	Sa_{1}
Quartz-Type silica	12	1.12 ±0.04	Sq_{12}
Colloidal silica	0.02	140*	$Sc_{0.02}$
Lanthanum oxide	<1	1.01 ±0.01	L

* Given by the provider

Both amorphous and crystalline silica have irregular and angular shapes. The amorphous silica has large particles, and its particle size distribution is generally not homogeneous (Figure 2(a)) (average particle size of 36 µm). The crystalline silica has a more homogeneous particle size distribution and a smaller particle size (approximately 12 µm), as shown in Figure 2(b) and Table 4. The amorphous silica of average size 1 µm obtained from grinding Sa_{36} is shown in Figure 2(c). The colloidal silica in Figure 2(d) has an estimated particle size of 22 nm. Meanwhile, La_2O_3 has a much smaller particle size (Figure 2(e)) than the amorphous Sa_{36} and crystalline

silica. However, lanthanum oxide has a strong tendency to form agglomerates with sizes up to 20 µm.

A temperature analysis reveals that amorphous silica initiates a phase transformation at 1200°C, where it presents a mixture of cristobalite and quartz. Crystalline silica retains the quartz structure up to 1200°C and subsequently evolves to the cristobalite variety after the treatment at 1500°C. At this temperature, both silicas have a cristobalite structure, but crystalline silica retains traces of quartz.

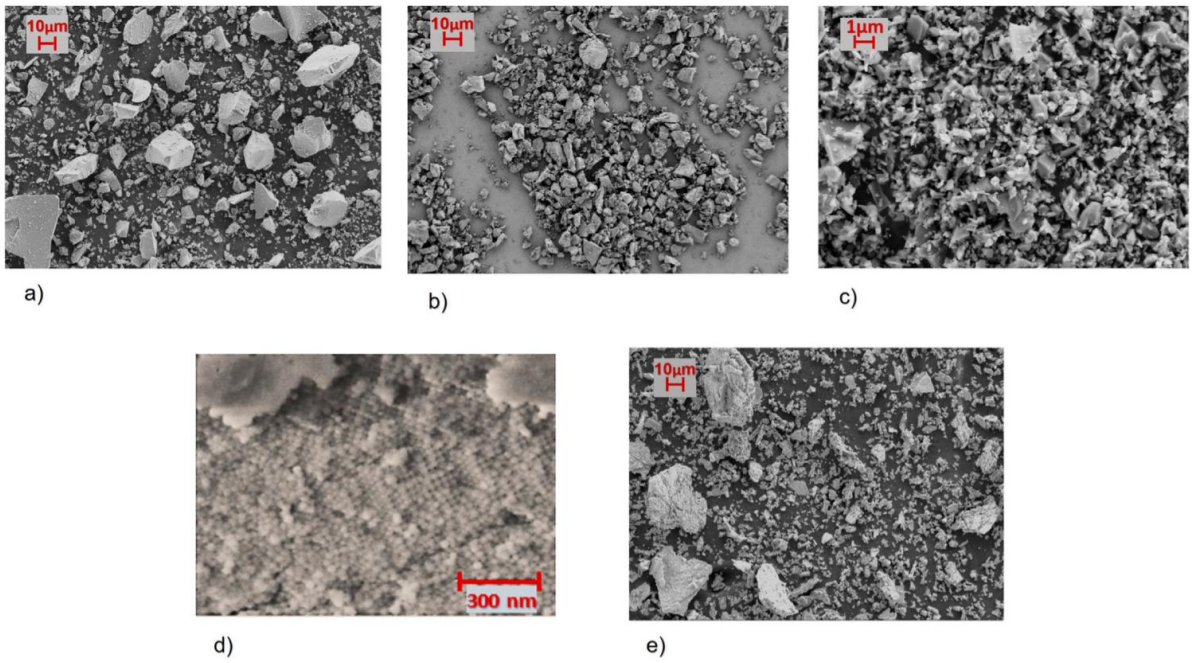

Figure 2. *SEM Micrographs of the starting powders (a) amorphous silica Sa36, (b) quartz-type silica Sq12, (c) amorphous silica Sa1, (d) colloidal silica Sc0.02 and (e) lanthanum oxide La2O3 (L).*

3.2.2. La_2SiO_5 synthesis at 1500°C

To evaluate the effect of the silica particle size on the lanthanum silicate formation, three average sizes of amorphous silica particles are used: 36 µm (Sa_{36}), 1 µm (Sa_1) and 0.02 µm (colloidal silica Sc). It is assumed that a smaller size of silica particles would increase the reactivity between reactive powders during the solid-state

reaction. The particle distribution of the mixtures (LS) of LSa_{36} and LSa_1 powders after attrition milling and $LSc_{0.02}$ after dispersion with ultrasonic waves are presented in the SEM micrographs of Figure 3. A better homogenization of the reagents is observed when silica particle size is smaller. In the mixed system LSa_{36} (Figure 3a), using the largest silica, some particles up to 10 µm remain and have not been ground. The reagent size ratio La:Si clearly increases from LSa_{36} to $LSc_{0.02}$.

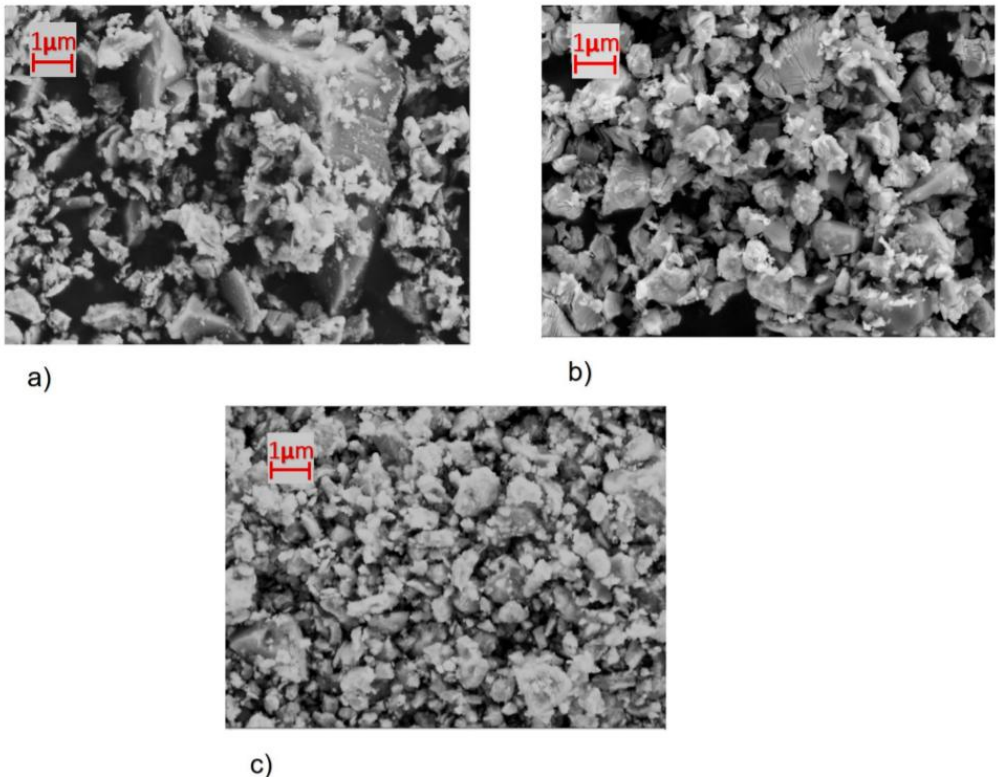

Figure 3. *Micrographs of samples after attrition milling, a) LSa36, b) LSa1 and after dispersion with ultrasonic waves c) LSc0.02.*

The XRD diagrams of the identified phases of these three powders, which were calcined at 1500°C for 10 h, and their quantification using Rietveld method are presented in Figure 4 and Table 5, respectively. La_2SiO_5 and apatite phases are the main phases that formed after 1500°C during 10 h. The apatite phase content

significantly decreases from 37.1%, 14.5% to 7.6% for LSa_{36}, LSa_1, and $LSc_{0.02}$ mixtures, respectively, when the size ratio La:Si increases. In contrast, the La_2SiO_5 phase content clearly increases from 46.65% and 80.1%, to 91.4% when the average silica particle size decreases, i.e., when the size ratio La:Si increases. Unreacted La_2O_3 impurities were identified in the XRD diagrams however, the amount of this reagent significantly decreases when the content of La_2SiO_5 increases. The La_2O_3 amount was only 1% (Vol%) in $LSc_{0.02}$ starting powder. Additionally, the $La_2Si_2O_7$ phase does not form when the silica particles are below 1 µm.

These results clearly show the high impact of the silica particle size on the La_2SiO_5 phase formation by solid-state reaction. A smaller silica particle size and a larger La_2O_3/SiO_2 size ratio enable better distribution and contact among the reagent particles during the mixing and synthesis process and promote a high purity level of the synthesized phase. When the silica presents a larger particle size (LSa_{36} starting powder, Figure 3a), large silica particles (up to 10 µm) remain in the mixture, even after the milling step, which induces low reactivity and poor homogeneity. This heterogeneity in the La:Si size ratio can cause local variations in the 1:1 molar ratio and promote the formation of secondary phases such as apatite and $La_2Si_2O_7$.

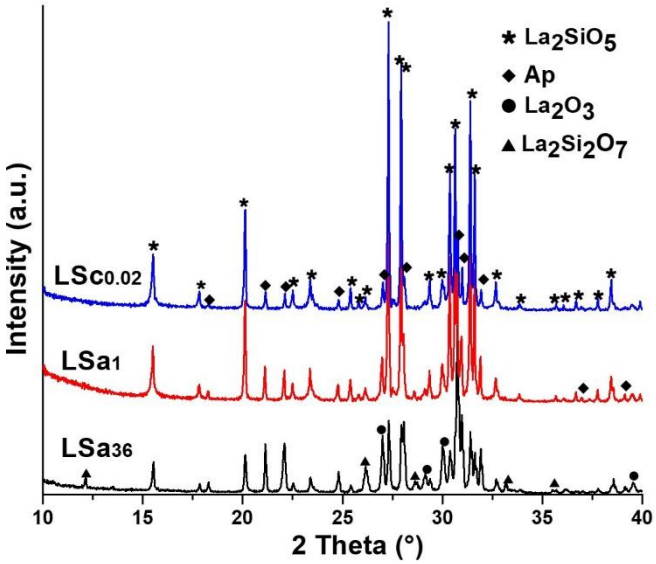

***Figure 4**. XRD patterns of LSa36, LSa1 and LSc0.02 samples calcined at 1500 °C/ 10 h.*

The effect of the particle size of the starting materials was proven by other authors, especially in the field of solid-state reaction from oxide precursors. For example, in the system of Y_2O_3-Al_2O_3 for the production of YAG phase [43], it has been reported that the particle size and size ratio of starting powders significantly affect the solid-state reaction pathways and final purity of the YAG phase. J.R. Gonzales et al. [44] studied the synthesis of cordierite from oxides such as SiO_2, MgO and Al_2O_3 and showed that reducing the particle size of the starting materials decreased the temperature at which the synthesis process started.

The results of the influence of the silica particle size on the purity of La_2SiO_5 by solid-state reaction show that to achieve a high degree of purity, the silica particle must be smaller than the La_2O_3 particles. A purity of 91.4% was obtained from the synthesis when colloidal silica was used. In this case, the particle size ratio La_2O_3/SiO_2 was the highest (1 µm/0.02 µm for the $LSc_{0.02}$ mixture). This result is satisfactory, and the synthesis process is quite simple compared to the long synthesis of other rare earth

silicates, where repeated grinding and calcination steps in 20-200 h are performed to obtain a single phase [13, 23–30].

3.3. Thermal analysis and in situ XRD at high temperature

To further study the La_2SiO_5 synthesis by solid-state reaction, thermal analysis and *in situ* XRD analysis at high temperature were performed to evaluate the reaction kinetics in three mixtures: LSa_{36}, LSa_1, and $LSc_{0.02}$.

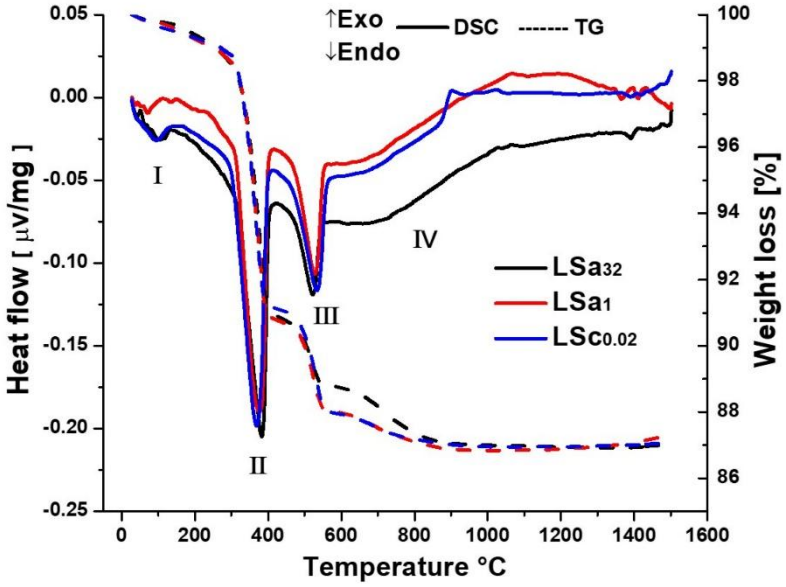

Figure 5. *TG/DSC analysis of starting mixture LSa36, LSa1 after milling and LSc0.02 after dispersion with ultrasonic waves.*

The dried powders obtained after attrition milling or ultrasonic dispersion were analyzed by TG/DSC (Figure 5). The mixture of powders presented four characteristic zones of temperature. The first one, which is below 200°C, (noted I in Figure 5) corresponds to the loss of water weakly adsorbed on the surface of the reagent powders. The second one between 300 and 400°C (noted II in Figure 5) corresponds to the decomposition of the $La(OH)_3$ and $La_2(OH)_4(CO_3)$ compounds

according to reactions 1 and 2. The hydroxide and hydroxycarbonate phases were previously formed by the reaction with atmospheric air or water in the milling stage. This evolution has been reported [22,45].

$$2La(OH)_3 \xrightarrow{310°C} 2\,LaOOH + 2\,H_2O \text{ (Eq.1)}$$

$$La_2(OH)_4(CO_3) \xrightarrow{430°C} La_2O_2(CO_3) + 2\,H_2O \text{ (Eq.2)}$$

The third temperature range of 500-650°C (noted III in Figure 5) corresponds to the LaOOH decomposition to form La_2O_3 (Eq.3).

$$2\,LaOOH \xrightarrow{460°C} La_2O_3 + H_2O \text{ (Eq.3)}$$

The last zone above 650°C (noted IV in Figure 5) corresponds to the decarbonation of $La_2O_2CO_3$ intermediate phase that formed according to Equation 2. This reaction is associated with a CO_2 gaseous release (Eq. 4).

$$La_2O_2(CO_3) \xrightarrow{650°C} La_2O_3 + CO_2$$

The thermal analysis results show that the three powder mixtures have similar behaviors below 600°C. In zone IV, at high temperatures, an exothermic peak is clearly observed at approximately 900-1000°C for the $LSc_{0.02}$ mixture, and a less intense exothermic peak at approximately 1000°C is identified for LSa_1, which may be related to the beginning crystallization of lanthanum silicate phases.

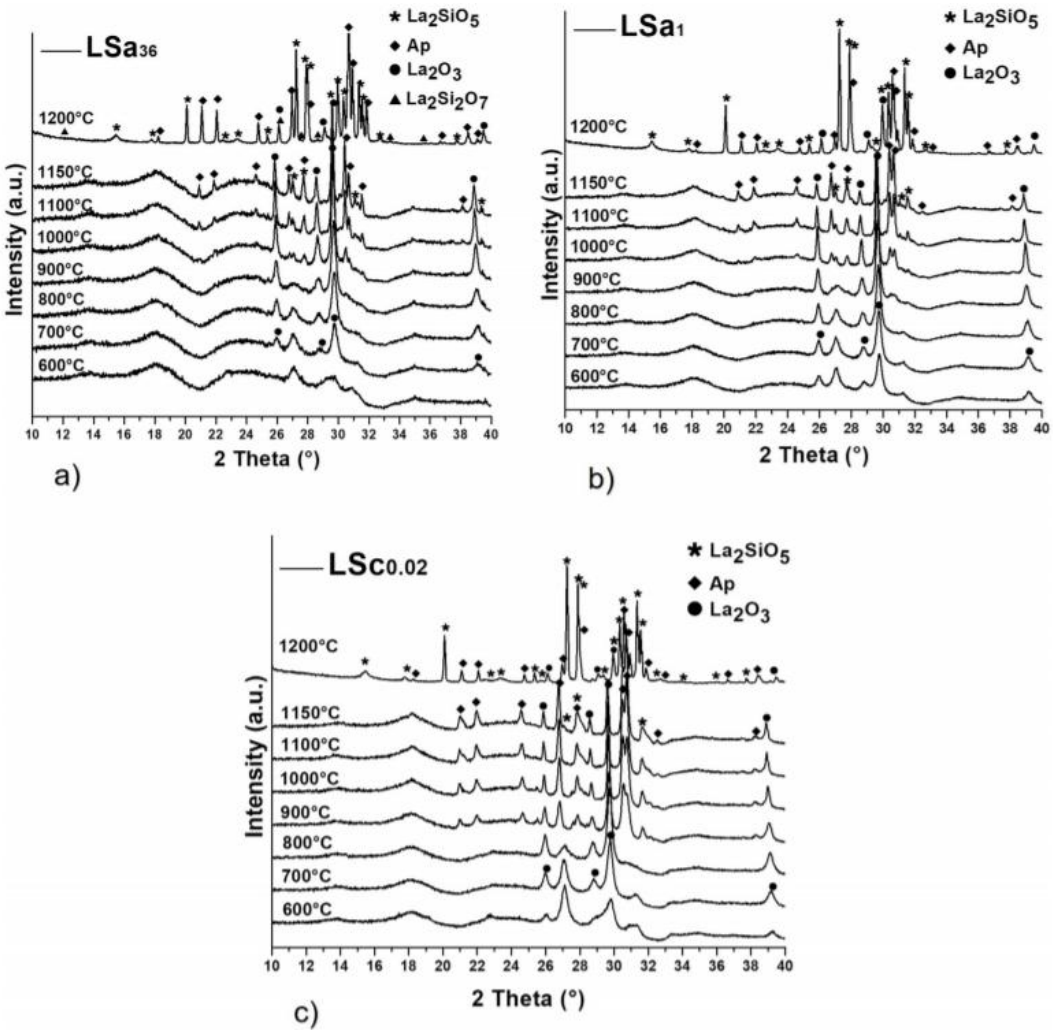

***Figure 6**. In-situ high temperature XRD of the samples a) LSa36, b) LSa1 and c) LSc0.02.*

In situ XRD diagrams obtained during the heating of powder mixtures from 600°C to 1150°C are shown in Figure 6. XRD diagrams obtained on powders calcined at 1200°C/10 h are added in the same figure. In all three samples, the formations of La_2SiO_5 and the apatite phases simultaneously occur, probably since there is a strong link between them, which are actually close in the phase diagram [1]. Moreover, the initial crystallization of an apatite phase $La_{4.67}(SiO_4)_3O$ is related to an intermediate product that forms in the La_2O_3-SiO_2 system, which is favorable for the subsequent yield of La_2SiO_5 [4]. The crystallization temperature of these phases

depends on the particle size of the silica starting powder: 1000°C for LSa_{36}, LSa_1 and 900°C for $LSc_{0.02}$. The data were analyzed by Rietveld method to quantify the apatite and La_2SiO_5 phases with respect to the temperature increase (Figure 7). The quantitative analysis of these phases clearly shows that an apatite phase predominates below 1200°C. However, at this temperature, the La_2SiO_5 phase ratio increases in comparison with the apatite phase ratio, so apatite may be transformed into La_2SiO_5 when the silica particles have a small diameter. In all cases, the $La_2Si_2O_7$ phase crystallization is not observed during heating from 600°C to 1150°C, which indicates that this phase is exclusively formed at high temperatures and only with a large diameter of silica particles.

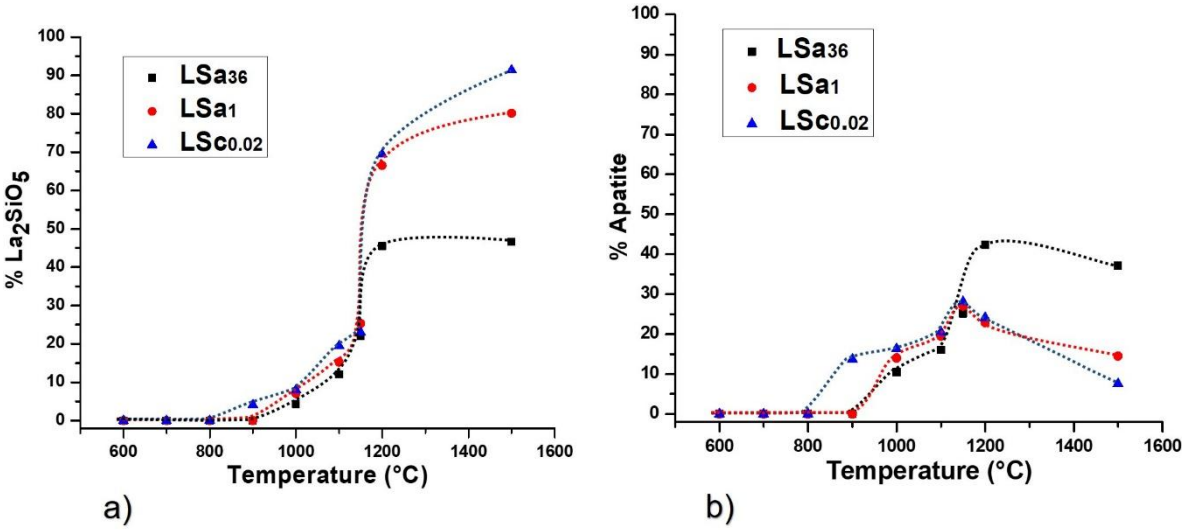

Figure 7. *Evolution during heating of a) La2SiO5 and b) Apatite for LSa36, LSa1 and LSc0.02 samples.*

The quantitative analysis of phase formation (Figure 7) confirms that an increase in La_2O_3/SiO_2 size ratio promotes the formation of the La_2SiO_5 phase instead of secondary phases above 1200°C. The decrease in silica particle size also improves the reaction kinetics or phasing crystallization rate and is the key parameter to favor La_2SiO_5 instead of apatite.

Actually, this study and others have shown the tendency of the apatite phase to crystallize more easily than other phases in the La_2O_3-SiO_2 system. In the field of TBCs (Thermal Barrier Coatings) and EBCs (Environmental barrier Coatings), for example, the contact of rare earth oxides with molten silica debris (CMAS: calcium – magnesium – aluminum - silicon systems) at high temperature generally leads to the formation of an oxyapatite phase, which is faster than other rare-earth (RE) silicates. The effect of the particle size was also observed with an increase in energetic stability with respect to enthalpy formation when the ionic radius of the RE increases [46–49]. Since La^{3+} presents the largest ionic radius (1.15 Å) among all rare earth elements, we assume that it explains its crystallization and temperature stability in the La_2O_3/SiO_2 system and the difficulty to obtain La_2SiO_5 as a pure phase.

The thermal analysis results are reasonably consistent with the high-temperature XRD results. A clear exothermic DSC peak can be distinguished at approximately 900°C for the $LSc_{0.02}$ sample (Figure 5) and correspond to the crystallization of the lanthanum silicate phases reported in *in situ* XRD (Figure 6). A less intense exothermic DSC peak at approximately 1000°C for LSa_1 is also observed. The crystallization peaks are not observed in LSa_{36}, which may be related to the larger silica particle size, which can reduce the reaction rate (see Figure 6). This can explain why the phase crystallization begins at a higher temperature and their crystallization is slower, which remains imperceptible during the thermal analysis by DSC, as shown in Figure 5 for LSa_{36}.

3.4. Mechanisms of formation of La_2SiO_5, apatite and $La_2Si_2O_7$ phases in the solid-state reaction of La_2O_3 and SiO_2

Based on previous analyses of *in situ* high-temperature XRD (Figure 6) and thermal analysis (TG-DSC, (Figure 5)), some mechanisms are proposed to explain the lanthanum silicates formation through the solid-state reaction of La_2O_3 and SiO_2 (Figure 8). Two cases are considered according to the La_2O_3/SiO_2 size ratio.

The first case (case I) corresponds to the LSa_{36} system, where SiO_2 particles are larger than La_2O_3 particles (small La:Si size ratio). In that case, we hypothesize that the large SiO_2 particles are surrounded by La_2O_3 particles. The second case (case II) corresponds to the $LSc_{0.02}$ sample, where the SiO_2 particles are smaller than the La_2O_3 particles (high La:Si size ratio). In that case, it is assumed that a thin layer of colloidal silica particles cover the larger La_2O_3 particles.

These two cases are presented in Figure 8. It is supposed that La_2SiO_5, apatite and La_2SiO_7 will grow on the surface of silica or lanthanum particles according to case I or II by forming concentric shell structures. The evolution of different silicates from La_2O_3 to SiO_2 will progress depending on the stoichiometry (1:1 for La_2SiO_5, 1:1.5 for apatite, and 1:2 for $La_2Si_2O_7$, Figure 8).

The objective of this study was to obtain the highest purity of La_2SiO_5. The solid-state reaction depends on the diffusion of La^{3+}, Si^{4+}, and O^{2-} species in the formed phases. Unfortunately, diffusion studies of these ionic species through apatite, La_2SiO_5 or $La_2Si_2O_7$ phases have not been reported. Hence, it is truly difficult to predict the formation reaction that limits the La_2SiO_5 phase formation during the solid-state

reaction, and these mechanisms are the result of a thorough analysis of previous experimental data.

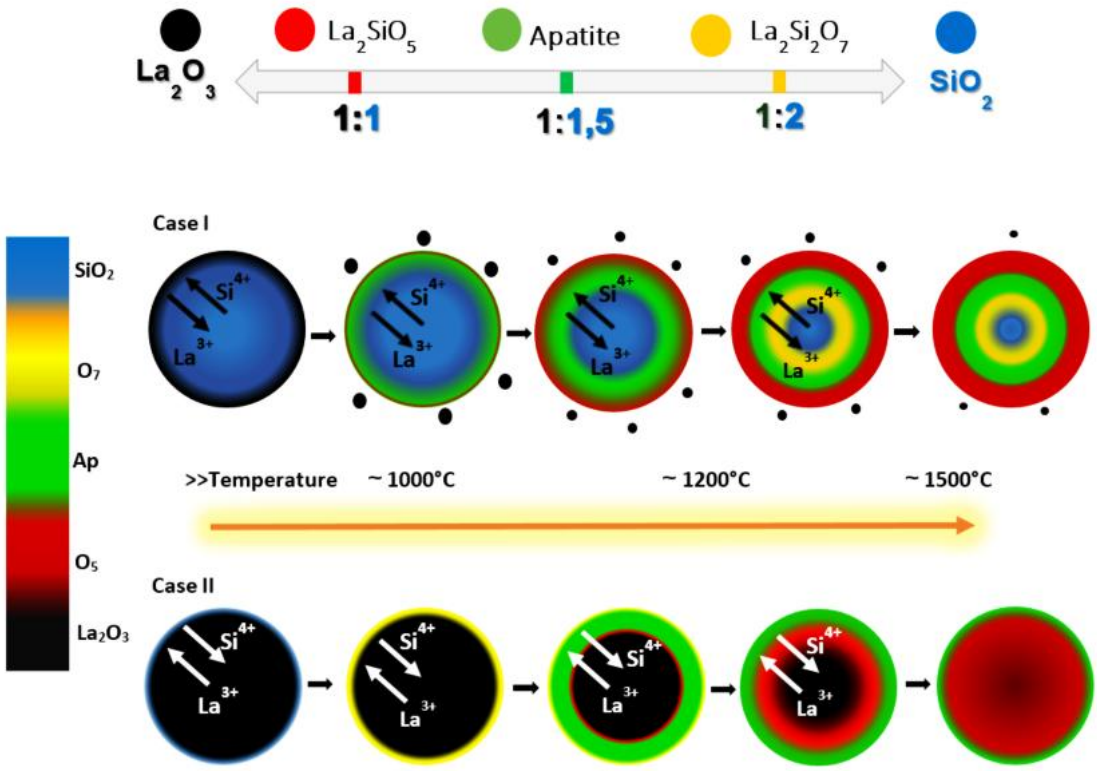

Figure 8. *Scheme of the solid state reaction of La_2O_3 and SiO_2 showing the evolution of the silicate phases with the temperature for two cases; case I: small size ratio - big particle size of SiO_2; case II: high size ratio - small particle size of SiO_2.*

In case I, at the beginning of the solid-state reaction, the simultaneous formation of the apatite and La_2SiO_5 phases are observed for the LSa_{36} system at 1000°C, and these phases progressively crystallize (Figures 6 and 7). It is assumed here that the La^{3+} species can easily progress through the heart of silica particles. This diffusion causes the joint formation of an apatite layer surrounded by a thin layer of La_2SiO_5 phase (on the richest side of La_2O_3). Both layers will progress into the heart of SiO_2 particles with the increase in temperature. At 1200°C, a small amount of $La_2Si_2O_7$ phase is detected from *in situ* XRD, which is attributed to the reaction at the interface

between the silica heart and the apatite layer (the Si^{4+} diffusion is assumed to be slower than the La^{3+} diffusion). At that temperature, La_2SiO_5 no longer forms, so the formation kinetic of this phase becomes very slow, while the $La_2Si_2O_7$ content increases. Hence, $La_2Si_2O_7$ is acting as a diffusion barrier and limits the diffusion of Si^{4+} species from the heart of the particle. At the end of the synthesis (1500°C/10 h, Figure 4), an equivalent amount of apatite and La_2SiO_5 is obtained, and there is unreacted La_2O_3 (represented in the scheme by small black points surrounding the core shell structure), which could not react with the silica from the heart due to the $La_2Si_2O_7$ blocking phase.

In case II, the small particle size of the silica leads to a better interaction between silica and lanthanum oxide, which accelerates the reaction kinetics and La_2SiO_5 phase formation. In this synthesis, a complete consumption of the reagents was observed, and the $La_2Si_2O_7$ secondary phase was not detected. This configuration enables a better interdiffusion of species. Thus, a thin layer of $La_2Si_2O_7$ (not detected in XRD) is quickly formed at the surface of the La_2O_3 particles due to the diffusion of La^{3+} species in colloidal silica. In this case, the $La_2Si_2O_7$ layer thickness will be limited by the very small diameter of SiO_2 particles (0.02 µm), and the thin $La_2Si_2O_7$ layer cannot limit the diffusion of Si^{4+} ions, unlike case I. This layer will be consumed to form the apatite phase; then, the La_2SiO_5 phase via the La^{3+} diffusion in lanthanum silicate phases is formed at the surface. La^{3+} ions can easily migrate throughout the particle and form the predominant La_2SiO_5 phase at the end of the diffusion and reaction.

Indeed, the maximal thickness of the $La_2Si_2O_7$ phase layer in all cases corresponds to the radius of silica particles, which can be associated with the usual notion of critical diffusion distance of the solid-state reaction at high temperature [34]. The

kinetic of solid-state reaction and formation of the La_2SiO_5 phase at high temperature are directly governed by the radius of silica particles starting powder. When the radius of silica particles is small, the $La_2Si_2O_7$ layer thickness is low, and the formation kinetic of La_2SiO_5 is sufficiently fast. In the opposite case, when the radius of silica particles is very large (several microns), the $La_2Si_2O_7$ layer is thick, and the formation kinetic of La_2SiO_5 phase or diffusion kinetics of chemical species at solid state becomes progressively slow because of the kinetic barrier created by $La_2Si_2O_7$.

4. Conclusion

The synthesis of La_2SiO_5 by the solid-state reaction between La_2O_3 and SiO_2 mixed in a 1:1 molar ratio was studied. The nature of silica (amorphous or crystalline) and its particle size (from several microns to colloidal silica at approximately 0.02 µm) greatly affect the crystallization kinetics and consequently the purity of the final material. Amorphous silica and a size ratio La_2O_3/SiO_2: 1 µm/0.02 µm enabled us to obtain the highest purity of La_2SiO_5 (91.4% was achieved at a temperature of 1500°C for 10 h) with a high degree of reproducibility.

A thorough *in situ* XRD analysis in a large range of temperature shows two opposite cases depending on the particle size of the silica. The most important parameter to promote the formation of La_2SiO_5 is certainly to enable the Si^{4+} diffusion through the lanthanum silicate phases (apatite and $La_2Si_2O_7$). Thus, by decreasing the silica particle size, the formation of the $La_2Si_2O_7$ layer can be limited or avoided, whereas when silica particles present a large diameter, a thick layer of $La_2Si_2O_7$ is formed, which acts as a diffusion barrier and limits the conversion into La_2SiO_5.

Acknowledgements

The authors wish to thank Dr. Jenny Jouin and Dr. Richard Mayet for their scientific and technical help, particularly in the Rietveld and high-temperature X-ray diffraction analyses.

References

[1] N.A. Toropov, I.A. Bondar, Silicates of rare-earth elements, Bull. Acad. Sci. USSR Div. Chem. Sci. 10 (1961) 682–687, https://doi.org/10.1007/BF00905927.

[2] F. Jiang, L. Cheng, H. Wei, Y. Wang, Hot corrosion behavior of Lu_2SiO_5 and La_2SiO_5 in a molten Na_2SO_4 environment : a first-principles corrosion resistance investigation, Ceram. Int. 45 (2019) 15532–15537, https://doi.org/10.1016/j.ceramint.2019.05.058.

[3] B.V.D. Nataliya, L. Minkova, Dimitr S. Todorovsky, Syhtesis of La_2SiO_5 and its separation from La_2O_3, Lanthan. Actinide Res. 3 (1991) 391–395.

[4] G. Tzvetkov, N. Minkova, Mechanochemically induced formation of La_2SiO_5, J. Mater. Sci. 35 (2000) 2435–2441, https://doi.org/10.1023/A:1004705332191.

[5] K. Fukuda, T. Iwata, E. Champion, Crystal structure of lanthanum oxyorthosilicate, La_2SiO_5, Powder Diffr. 21 (2006) 300–303, https://doi.org/10.1154/1.2383066.

[6] J. Felsche, The crystal chemistry of the rare-earth silicates, Struct. Bond, 1973, pp.99–197, https://doi.org/10.1007/3-540-06125-8_3.

[7] M. Leskela, K. Jyrkas, Effect of flux materials on the reaction of Y_2O3 and SiO_2, J. Am. Ceram. Soc. 70 (1987) 160–161, https://doi.org/10.1111/j.1151-2916.1987.tb05695.x.

[8] K. Fukuda, T. Asaka, R. Hamaguchi, T. Suzuki, H. Oka, A. Berghout, E. Béchade, O. Masson, I. Julien, E. Champion, P. Thomas, Oxide-Ion conductivity of highly caxis oriented apatite-type lanthanum silicate polycrystal formed by reactive diffusion between La_2SiO_5 and $La_2Si_2O_7$, Chem. Mater. 23 (2011) 5474–5483, https://doi.org/10.1021/cm2029905.

[9] K. Fukuda, R. Watanabe, M. Oyabu, R. Hasegawa, T. Asaka, H. Yoshida, Oxide-Ion conductivity enhancement of polycrystalline lanthanum silicate oxyapatite induced by BaO doping and grain alignment, Cryst. Growth Des. 16 (2016) 4519–4525, https://doi.org/10.1021/acs.cgd.6b00638.

[10] K. Fukuda, T. Asaka, S. Hara, M. Oyabu, A. Berghout, E. Béchade, O. Masson, I. Julien, P. Thomas, Crystal structure and oxide-ion conductivity along c-axis of Si deficient apatite-type lanthanum silicate, Chem. Mater. 25 (2013) 2154–2162, https://doi.org/10.1021/cm400892p.

[11] K. Fukuda, R. Hasegawa, T. Kitagawa, H. Nakamori, T. Asaka, A. Berghout, E. Béchade, O. Masson, J. Jouin, P. Thomas, Well-aligned polycrystalline lanthanum silicate oxyapatite grown by reactive diffusion between solid La_2SiO_5 and gases [$SiO+1/2O_2$], J. Solid State Chem. (2016), https://doi.org/10.1016/j.jssc.2015.12.007.

[12] S. Ide, H. Takahashi, I. Yashima, K. Suematsu, K. Watanabe, K. Shimanoe, Effect of boron substitution on oxide-ion conduction in c-axis-oriented apatite-type lanthanum silicate, J. Phys. Chem. C 124 (2020) 2879–2885, https://doi.org/10.1021/ acs.jpcc.9b11454.

[13] A.N. Christensen, R.G. Hazell, A.W. Hewat, M. Fondo, E. Gómez-Fórneas, C.A. McAuliffe, S. Styring, C. Tommos, K. Warncke, B.R. Wood, Synthesis, crystal growth and structure investigations of rare-earth disilicates and rare-earth oxyapatites, Acta Chem. Scand. 51 (1997) 37–43, https://doi.org/10.3891/acta.chem.scand.51-0037.

[14] K. Fukuda, T. Iwata, E. Champion, Crystal Structure of Lanthanum Oxyorthosilicate, La_2SiO_5, 2006, p. 2383066, https://doi.org/10.1154/1.2383066.

[15] N.I. Leonyuk, E.L. Belokoneva, G. Bocelli, L. Righi, E.V. Shvanskii, R.V. Henrykhson, N.V. Kulman, D.E. Kozhbakhteeva, Crystal growth and structural refinements of the Y_2SiO_5, $Y_2Si_2O_7$ and $LaBSiO_5$ single crystals, Cryst. Res. Technol. 34 (1999) 1175–1182, https://doi.org/10.1002/(SICI)1521-4079 199911) 34:9 < 1175::AID-CRAT1175 > 3.0.CO;2-2.

[16] K. Kobayashi, K. Hirai, T.S. Suzuki, T. Uchikoshi, T. Akashi, Y. Sakka, Sinterable powder fabrication of lanthanum silicate oxyapatite based on solid-state reaction method, J. Ceram. Soc. Japan. 123 (2015) 274–279, https://doi.org/10.2109/jcersj2.123.274.

[17] M. Sakao, T. Ishihara, H. Yoshioka, Fabrication and ionic conductivity of oriented lanthanum silicate films with apatite-type structure, Solid State Ionics 293 (2016) 51–55, https://doi.org/10.1016/j.ssi.2016.05.018.

[18] K. Fukuda, T. Asaka, T. Uchida, Thermal expansion of lanthanum silicate oxyapatite ($La_{9.33+2x}(SiO_4)_6O_{2+3x}$), lanthanum oxyorthosilicate (La_2SiO_5) and lanthanum sorosilicate ($La_2Si_2O_7$), J. Solid State Chem. (2012), https://doi.org/10.1016/j.jssc.2012.04.043.

[19] H. Meradi, L. Atoui, L. Bahloul, K. Boubendira, A. Bouazdia, F. Ismail, Characterization by thermal analysis of natural kieselguhr and sand for industrial application, Energy Procedia 74 (2015) 1282–1288, https://doi.org/10.1016/j.egypro.2015.07.773.

[20] C.D. Brandle, A.J. Valentino, G.W. Berkstresser, Czochralski growth of rare-earth orthosilicates (Ln_2SiO_5), J. Cryst. Growth 79 (1986) 308–315, https://doi.org/10.1016/0022-0248(86)90454-9.

[21] S. Nakayama, T. Kageyama, H. Aono, Y. Sadaoka, Ionic conductivity of lanthanoid silicates, $Ln_{10}(SiO_4)_6O_3$ (Ln = La, Nd, Sm, Gd, Dy, Y, Ho, Er and Yb), J. Mater. Chem. 5 (1995) 1801, https://doi.org/10.1039/jm9950501801.

[22] E. Béchade, I. Julien, T. Iwata, O. Masson, P. Thomas, E. Champion, K. Fukuda, Synthesis of lanthanum silicate oxyapatite materials as a solid oxide fuel cell electrolyte, J. Eur. Ceram. Soc. 28 (2008) 2717–2724, https://doi.org/10.1016/j.jeurceramsoc.2008.03.045.

[23] H. Yoshioka, S. Tanase, Magnesium doped lanthanum silicate with apatite-type structure as an electrolyte for intermediate temperature solid oxide fuel cells, Solid State Ionics 176 (2005) 2395–2398, https://doi.org/10.1016/j.ssi.2005.06.026.

[24] J.E.H. Sansom, J.R. Tolchard, M.S. Islam, D. Apperley, P.R. Slater, Solid state 29Si NMR studies of apatite-type oxide ion conductors, https://doi.org/10.1039/b600122j, (2006).

[25] E. Kendrick, M. Islam, P. Slater, Investigation of the structural changes on Zn doping in the apatite-type oxide ion conductor $La_{9.33}Si_6O_{26}$: a combined neutron diffraction and atomistic simulation study, Solid State Ionics 177 (2007) 3411–3416, https://doi.org/10.1016/j.ssi.2006.10.013.

[26] A. Mineshige, H. Hayakawa, T. Nishimoto, A. Heguri, T. Yazawa, Y. Takayama, Y. Kagoshima, H. Takano, S. Takeda, J. Matsui, Preparation of lanthanum silicate electrolyte with high conductivity and high chemical stability, Solid State Ionics 319 (2018) 223–227, https://doi.org/10.1016/j.ssi.2018.02.002.

[27] J.E.H. Sansom, P.R. Slater, The synthesis and conductivities of the apatite-type phases $La_{9.33}Si_{6-X}GexO_{26}$, Solid State Phenom. 90–91 (2003) 189–194 https://doi.org/10.4028/www.scientific.net/ssp.90-91.189.

[28] H. Okudera, Y. Masubuchi, S. Kikkawa, A. Yoshiasa, Structure of oxide ion-conducting lanthanum oxyapatite, $La_{9.33}(SiO_4)_6O_2$, Solid State Ionics 176 (2005) 1473–1478, https://doi.org/10.1016/j.ssi.2005.02.014.

[29] J. Sansom, Synthesis and structural characterisation of the apatite-type phases $La_{10-x}Si_6O_{26+z}$ doped with Ga, Solid State Ionics 167 (2004) 17–22, https://doi.org/10.1016/j.ssi.2003.12.014.

[30] J.E.H. Sansom, P.R. Slater, Oxide ion conductivity in the mixed Si/Ge apatite-type phases La9.33Si6-xGexO26, Solid State Ionics 167 (2004) 23–27, https://doi.org/10.1016/j.ssi.2003.12.015.

[31] A. Pons, J. Jouin, E. Béchade, I. Julien, O. Masson, P.M. Geffroy, R. Mayet, P. Thomas, K. Fukuda, I. Kagomiya, Study of the formation of the apatite-type phases $La_{9.33+x}(SiO_4)_6O_{2+3x/2}$ synthesized from a lanthanum oxycarbonate $La_2O_2CO_3$, Solid State Sci. 38 (2014) 150–155, https://doi.org/10.1016/j.solidstatesciences.2014.10.013.

[32] F. Jiang, L. Cheng, H. Wei, Y. Wang, Hot corrosion behavior of Lu_2SiO_5 and La_2SiO_5 in a molten Na_2SO_4 environment: a first-principles corrosion resistance investigation, Ceram. Int. 45 (2019) 15532–15537, https://doi.org/10.1016/j.ceramint.2019.05.058.

[33] W. Liu, S. Yamaguchi, T. Tsuchiya, S. Miyoshi, K. Kobayashi, W. Pan, Sol–gel synthesis and ionic conductivity of oxyapatite-type $La_{9.33+x}Si_6O_{26+1.5x}$, J. Power Sources 235 (2013) 62–66, https://doi.org/10.1016/j.jpowsour.2013.01.194.

[34] K. Kobayashi, T.S. Suzuki, T. Uchikoshi, Y. Sakka, Low-temperature formation of Ln silicate oxyapatite (Ln=La and Nd) by the water-based sol–gel method, Solid State Ionics 204–205 (2011) 91–96, https://doi.org/10.1016/j.ssi.2011.10.011.

[35] S. Célérier, C. Laberty-Robert, J.W. Long, K.A. Pettigrew, R.M. Stroud, D.R. Rolison, F. Ansart, P. Stevens, Synthesis of $La_{9.33}Si_6O_{26}$ pore–solid nanoarchitectures via epoxide-driven sol–gel chemistry, Adv. Mater. 18 (2006) 615–618, https://doi.org/10.1002/adma.200501938.

[36] G. Tzvetkov, N. Minkova, Mechanochemical Stimulation of the Synthesis of Lanthanum Oxyapatite, (1999), pp. 354–358, https://doi.org/10.1016/S0167-577X(99)00034-8.

[37] A.F. Fuentes, L. Takacs, Preparation of multicomponent oxides by mechanochemical methods, J. Mater. Sci. 48 (2013) 598–611, https://doi.org/10.1007/s10853-012-6909-x.

[38] V. V Zyryanov, Mechanochemical Synthesis of Complex Oxides vol. 105, (2008), https://doi.org/10.1070/RC2008v077n02ABEH003709.

[39] M. Shinozaki, M. Senna, Effects of number and size of milling balls on the mechanochemical activation of fine crystalline solids, Ind. Eng. Chem. Fundam. 20 (1981) 59–62, https://doi.org/10.1021/i100001a011.

[40] M. Senna, Incipient chemical interaction between fine particles under mechanical stress a feasibility of producing advanced materials via mechanochemical routes, Solid State Ionics (1993) 63–65, https://doi.org/10.1016/0167-2738(93)90078-H 3–9.

[41] M. Senna, Recent development of materials design through a mechanochemical route, Int. J. Inorg. Mater. 3 (2001) 509–514, https://doi.org/10.1016/S1466-6049(01)00060-5.

[42] V. Devedzic, Introduction to soft mechanochemistry, Soft Mechanochemical Synth, Kluwer Academic Publishers, Boston, 2006, pp. 1–8, , https://doi.org/10.1007/0-306-47646-0_1.

[43] E.R. Kupp, S. Kochawattana, S.-H. Lee, S. Misture, G.L. Messing, Particle size effects on yttrium aluminum garnet (YAG) phase formation by solid-state reaction, J. Mater. Res. 29 (2014) 2303–2311, https://doi.org/10.1557/jmr.2014.224.

[44] J.R. González-Velasco, R. Ferret, R. López-Fonseca, M.A. Gutiérrez-Ortiz, Influence of particle size distribution of precursor oxides on the synthesis of cordierite by solid-state reaction, Powder Technol. 153 (2005) 34–42, https://doi.org/10.1016/j.

[45] S. Bernal, F.J. Botana, R. García, J.M. Rodríguez-Izquierdo, Thermal evolution of a sample of La_2O_3 exposed to the atmosphere, Thermochim. Acta 66 (1983) 139–145, https://doi.org/10.1016/0040-6031(93)85026-6.

[46] G. Costa, B.J. Harder, V.L. Wiesner, D. Zhu, N. Bansal, K.N. Lee, N.S. Jacobson, D. Kapush, S.V. Ushakov, A. Navrotsky, Thermodynamics of reaction between gas-turbine ceramic coatings and ingested CMAS corrodents, J. Am. Ceram. Soc. 102 (2018) 1–17, https://doi.org/10.1111/jace.16113.

[47] G. Costa, B.J. Harder, N.P. Bansal, B.A. Kowalski, J.L. Stokes, Thermochemistry of calcium rare-earth silicate oxyapatites, J. Am. Ceram. Soc. 103 (2020) 1446–1453, https://doi.org/10.1111/jace.16816.

[48] A.S. Risbud, K.B. Helean, M.C. Wilding, P. Lu, A. Navrotsky, Enthalpies of formation of lanthanide oxyapatite phases, J. Mater. Res. 16 (2001) 2780–2783, https://doi.org/10.1557/JMR.2001.0381.

[49] D.L. Poerschke, R.W. Jackson, C.G. Levi, Silicate deposit degradation of engineered coatings in gas turbines: progress toward models and materials solutions, Annu. Rev. Mater. Res. 47 (2017) 297–330, https://doi.org/10.1146/annurev-matsci010917-105000.